Sequestration of GPI-Anchored Proteins in Caveolae Triggered by Cross-Linking

Satyajit Mayor, Karen G. Rothberg, Frederick R. Maxfield*

Glycosyl-phosphatidylinositol (GPI)–anchored proteins have been reported to reside in clusters collected over small membrane invaginations called caveolae. The detection of different GPI-anchored proteins with fluorescently labeled monoclonal antibodies showed that these proteins are not constitutively concentrated in caveolae; they enter these structures independently after cross-linking with polyclonal secondary antibodies. Analysis of the cell surface distribution of the GPI-anchored folate receptor by electron microscopy confirms these observations. Thus, multimerization of GPI-anchored proteins regulates their sequestration in caveolae, but in the absence of agents that promote clustering they are diffusely distributed over the plasma membrane.

A diverse set of eukaryotic proteins including cell surface receptors, enzymes, and adhesion molecules have a lipid modification involving the replacement of a carboxyl-terminal peptide sequence with a GPI moiety that serves as a membrane anchor (*1*). Proteins anchored by GPI have been reported to be clustered at the cell surface, and a significant fraction of the clusters are localized to 60-nm membrane invaginations called caveolae that have been implicated in the transport of folate and other small molecules (potocytosis) and in intracellular signaling processes (*2*).

In previous studies, the localization of GPI-anchored proteins was determined with unlabeled primary polyclonal or monoclonal antibodies (mAbs) followed by labeled polyclonal secondary antibodies. To observe the native distribution of a GPI-anchored protein, the folate receptor, we directly conjugated the fluorophore Cy3 to a mAb (MOv19) (*3*) to the folate receptor. When G3G2 cells (3T3-L1 cells transfected with folate receptor) (*4*) were incubated with Cy3-labeled MOv19 (Cy3-MOv19) at 37°C for 8 min, the fluorescence was diffusely distributed over the cell surface (Fig. 1A). After the addition of an unlabeled polyclonal immunoglobulin G (IgG) antibody against the mAb, the fluorescence rapidly redistributed to a punctate pattern (Fig. 1B) that resembled the previously reported distributions of the GPI-anchored folate receptor (*5*, *6*).

This redistribution was not specific for transfected folate receptors in 3T3-L1 cells: Similar results were obtained for endogenous folate receptors in MA104 cells labeled with MOv19 and fixed before the immunoelectron microscopic detection of the mAb (Fig. 1C and Table 1). Treatment with secondary antibodies before fixation caused >90% of the immunolabeled folate receptors to redistribute into clusters (Fig. 1D and Table 1). As in previous studies, the clusters are often seen adjacent to invaginations (*5*, *6*). Quantitative analyses of the surface distribution of folate receptors (Table 1) show that there is no significant concentration of folate receptors in caveolae. However, after cross-linking there is a substantial enrichment of the antibody-induced clusters in caveolae. This enrichment is similar to previously reported values of clustered populations (*5*, *6*). We conclude that GPI-anchored folate receptors are not concentrated in caveolae to any significant extent in the absence of clustering agents.

The diffuse fluorescence of the Cy3-MOv19–labeled folate receptor was independent of the presence of folate because it was also observed in G3G2 and MA104 cells that had been grown in folate-deficient medium for 5 days and incubated in the presence (5 to 30 min at 37°C) or absence of 20 μM folic acid (MOv19 has no effect on the binding of folate to its receptor nor on the uptake of folic acid by the cell). In addition to the folate receptor in 3T3-L1, MA104, and CaCo-2 cells (Fig. 2A), two other GPI-anchored proteins, decay accelerating factor (DAF) and Thy-1, detected by staining with fluorescently labeled mAbs, were also diffusely distributed on the surface of human umbilical vein endothelial cells (HUVECS) and 3T3-L1 cells, respectively (Fig. 2, B and C). The slight granularity detectable at the cell surface is probably due to the presence of GPI-anchored proteins on microvilli at the cell surface. As with the folate receptor (Figs. 1, B and D, and 2E), the addition of unlabeled polyclonal secondary IgG antibody caused the redistribution of Thy-1 and DAF into punctate foci (Fig. 2, F and G).

The diffuse distribution of folate recep-

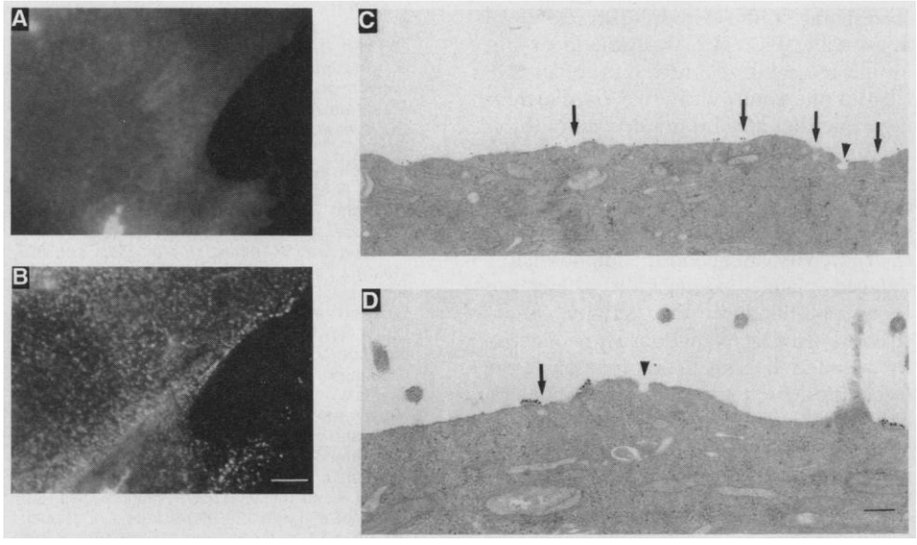

Fig. 1. Antibody-induced redistribution of folate receptor in living cells. (**A** and **B**) Cells of the 3T3-L1 line transfected with folate receptor (G3G2 cells) were incubated with Cy3-labeled mAb (10 μg/ml) to folate receptor (Cy3-MOv19) for 8 min at 37°C and rinsed three times in HF-BSA (*24*). The cells were then imaged (A) before and (B) 12 min after the addition of unlabeled polyclonal goat IgG against mouse mAb (final concentration of 20 μg/ml) to the cells as described (*24*) (scale bar, 10 μm). In control cells incubated for 12 min without the addition of polyclonal IgG, the fluorescence remained diffuse, as in (A). (**C** and **D**) Cells of the MA104 line (*25*) were incubated with Cy3-MOv19 (2 μg/ml) for 1 hour at 4°C, rinsed, and incubated for an additional 10 min at 37°C. The cells were then fixed with 3% paraformaldehyde and 0.5% glutaraldehyde for 30 min at room temperature (C) before or (D) after labeling with rabbit polyclonal serum against mouse IgG (20 μg/ml) followed by gold (10 nm)-labeled goat anti-rabbit IgG (2 μg/ml) and processed for electron microscopy (*25*). Arrows and arrowheads indicate structures identified as caveolae and coated pits, respectively (scale bar = 200 nm).

S. Mayor and F. R. Maxfield, Department of Pathology, College of Physicians and Surgeons, Columbia University, New York, NY 10032, USA.
K. G. Rothberg, Department of Cell Biology and Neuroscience, University of Texas Southwestern Medical Center, Dallas, TX 75235, USA.
*To whom correspondence should be addressed.

tor, DAF, and Thy-1 labeled with their respective fluorescent mAbs could be converted to a clustered distribution even if cells had been fixed for 20 min at 23°C in 3% paraformaldehyde before the addition of a cross-linking polyclonal secondary antibody or when fixed before being labeled with fluorescent mAbs followed by incubation with unlabeled secondary antibodies (Fig. 2, D and H). The ability of GPI-anchored proteins to redistribute after fixation in paraformaldehyde presumably accounts for the previously reported immunolocalizations of these proteins in tight clusters (5, 6). This redistribution was prevented by fixing for longer periods (>1 hour) or by the use of 0.3 to 0.5% glutaraldehyde along with 3% paraformaldehyde (Fig. 1, C and D). Because several specific mAbs bound to different GPI-anchored proteins showed a diffuse distribution, it is unlikely that the antibody treatments are artificially causing the dispersion of the GPI-anchored proteins. Furthermore, the diffuse distribution seen in cells fixed with glutaraldehyde before the addition of a second antibody supports the conclusion that sequestration in caveolae requires antibody-induced cross-linking.

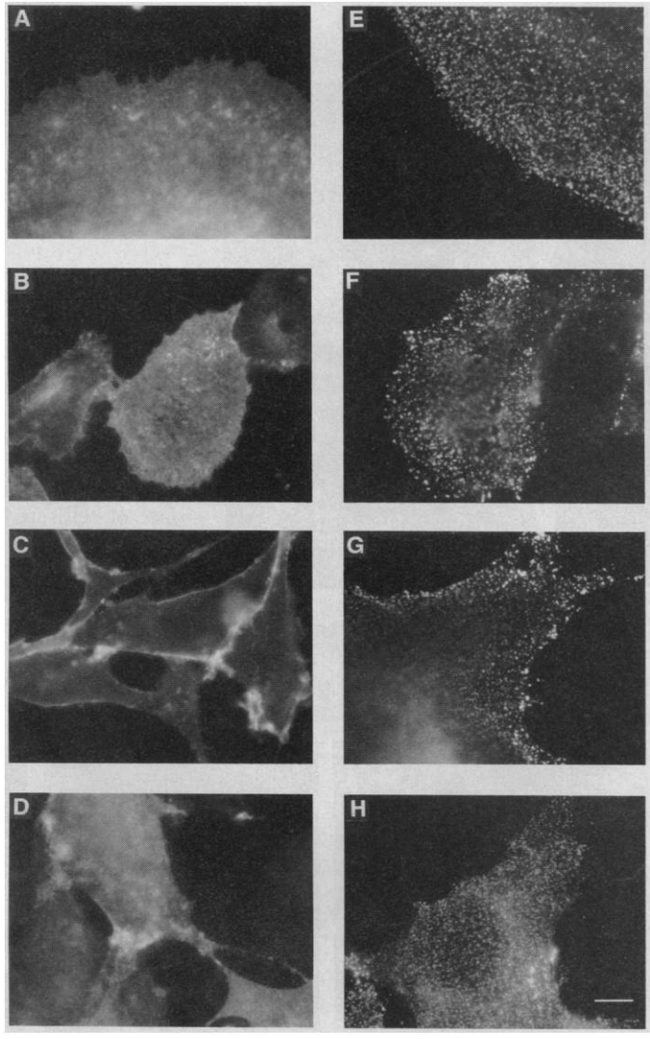

Fig 2. Surface distribution of GPI-anchored proteins. (**A** and **E**) Cells of the CaCo-2 line and (**B** and **F**) HUVECS stained with fluorescently labeled mouse monoclonal IgGs to the folate receptor and DAF, respectively (*26*). (**C, D, G,** and **H**) Cells of the 3T3-L1 line were stained with fluorescein-labeled rat mAb to Thy-1.2 [fluoroscein isothiocyanate (FITC) rat anti–Thy-1]. The cells were imaged (*24*), either (A to D) directly or (E to H) after treatment with appropriate polyclonal secondary antibodies to induce cross-linking of the primary antibody. In (D) and (H), 3T3-L1 cells were fixed for 20 min at room temperature with 3% paraformaldehyde, before staining with FITC anti–Thy-1. The occasional bright spots observed in panels A and B are probably due to the presence of microvilli on the surfaces of these cells (scale bar, 10 μm).

Multiple GPI-anchored proteins have been localized to a single caveola (5, 6). However, the cross-linking of a single GPI-anchored protein was not sufficient to cocluster other GPI-anchored proteins. In the absence of a secondary antibody, the folate receptor and Thy-1 were diffusely distributed over the cell surface (Figs. 1A and 2, A and C). The addition of a cross-linking polyclonal secondary IgG specific for the mouse mAb (that is, the anti-folate receptor mAb) redistributed the folate receptor fluorescence into punctate foci, whereas the diffuse nature of the Thy-1 distribution was unaltered (Fig. 3, A and B). Similarly, the diffuse distribution of the folate receptor was unaltered if Thy-1 was clustered with a polyclonal secondary IgG against rat monoclonal to Thy-1. The sequential addition of cross-linking polyclonal IgG specific for the rat monoclonal IgG to cells treated as shown in Fig. 3, A and B, caused the Thy-1 fluorescence to redistribute into punctate foci (Fig. 3, C and D). The observation that cross-linking of one GPI-anchored protein is not sufficient to cause others to cocluster with it shows that GPI-anchored proteins are independently recruited into punctate foci. This observation also suggests that there is no significant association among multiple GPI-anchored proteins.

A significant fraction of the Thy-1 clusters colocalized with the previously formed folate receptor clusters (Fig. 3, C and D). Similar coclustering of DAF and folate receptors was observed in CaCo-2 cells after the cross-linking of the DAF molecules with appropriate polyclonal secondary antibodies (Fig. 4, A to C). The extent of colocalization of folate receptor clusters with DAF, apparent from the large number of yellow foci seen in Fig. 4C, was quantified by digital image processing (*7*). About 75% of folate receptor clusters contained

Table 1. Quantitative analyses of the distribution of folate receptors on MA104 cells. Cells were processed for electron microscopy as described in Fig. 1. Fifty- to sixty-nanometer sections were used for quantitative analyses. The analysis of negatives (×20,000 magnification) was carried out with a ×10 ocular lens. More than 50 negatives of randomly selected fields were analyzed for each condition in each experiment (*27*).

Experiment (condition)	Membrane length (μm)	Number of caveolae	Number of coated pits	Number of gold particles	Percent gold particles in clusters (number of clusters)	Percent gold particles associated with caveolae (relative concentration)	Percent gold particles associated with coated pits (relative concentration)
1 (pre-fix)	256	49	49	576	9.9 (13)	2.6 (0.9)	7.1 (1.5)
2 (pre-fix)	228	37	40	522	2.9 (4)	5.2 (2.1)	5.9 (1.4)
1 (post-fix)	250	35	32	478	90.4 (46)	23.6 (11.3)	3.8 (1.2)
2 (post-fix)	218	52	44	747	96.4 (58)	25.4 (7.1)	4.2 (0.8)

detectable DAF, and ~50% of DAF clusters colocalized with folate receptor clusters. These are well above random values for colocalization (*7*). A similar analysis (average values from five fields) of the coclustering of Thy-1 and folate receptors on G3G2 cells showed that ~35% of the folate receptor clusters contained detectable Thy-1 (random colocalization value of ~12%) and ~55% of Thy-1 clusters contained detectable folate receptor (random colocalization value of ~10%). Thus, although GPI-anchored protein monomers do not associate with each other, they do cocluster when cross-linked.

Caveolin, a 22-kD integral membrane protein, has been localized to the cytoplasmic surface of caveolae, indicating that it is a component of the caveolae membrane coat (*8*). There is significant colocalization of the folate receptor clusters with caveolin (Fig. 4, D to F). Quantitative analysis by digital image processing showed that ~50% of the folate receptor clusters colocalized with caveolin-labeled foci (random colocalization value of ~21%), while >65% of the caveolin-labeled foci contained folate receptors (random colocalization value of ~27%). The extent of the colocalization of folate receptor clusters with the caveolin staining pattern determined by fluorescence microscopy was higher than the percentage of clusters observed over caveolae by electron microscopy (Table 1). We attribute this difference to the lower resolution of optical microscopy and the possibility that caveolae in thin sections adjacent to clusters of colloidal gold would not have been detected in our electron microscopic analysis. The association of these clusters with caveolae appears to be specific, because it is dependent on the integrity of the caveolae and procedures that disrupt caveolae such as treatment with cholesterol-binding drugs (filipin and nystatin) or cholesterol depletion from the plasma membrane prevent the clustering of cross-linked folate receptors (*9*). An increase in the cholesterol to phospholipid ratio by procedures described previously (*10*), however, did not alter the diffuse distribution of GPI-anchored proteins in G3G2 cells as detected by fluorescently labeled primary mAbs.

Folate transport by potocytosis would require a high concentration of folate bound to receptors in caveolae (*2, 11*). However, our data show that folate receptors on the surface of cells are diffusely distributed, independently of the presence of folate, arguing strongly against the potocytosis model of folate uptake. The observation that GPI-anchored folate receptors are detected in coated pits at densities consistent with random association (Table 1) strongly suggests

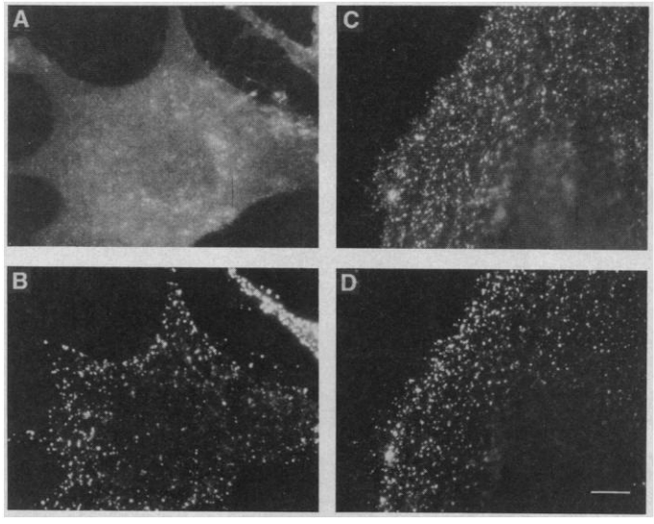

Fig. 3. Independent clustering of Thy-1 and folate receptor on the surface of G3G2 cells. Cells were stained with (**A** and **C**) FITC–rat anti-Thy-1 and (**B** and **D**) Cy3 mouse monoclonal IgG to folate receptor, Cy3-MOv19, as described (*24*). The cells were then either incubated with (A and B) polyclonal goat anti-mouse IgG (10 μg/ml) alone or (C and D) polyclonal anti-mouse IgG (10 μg/ml) followed by polyclonal goat anti-rat IgG (25 μg/ml) as described in the legend of Fig. 2. Images corresponding to (A and C) fluorescein and (B and D) Cy3 fluorescence were collected from the same field with imaging equipment for dual-label fluorescence microscopy as described (*13*) (scale bar, 10 μm).

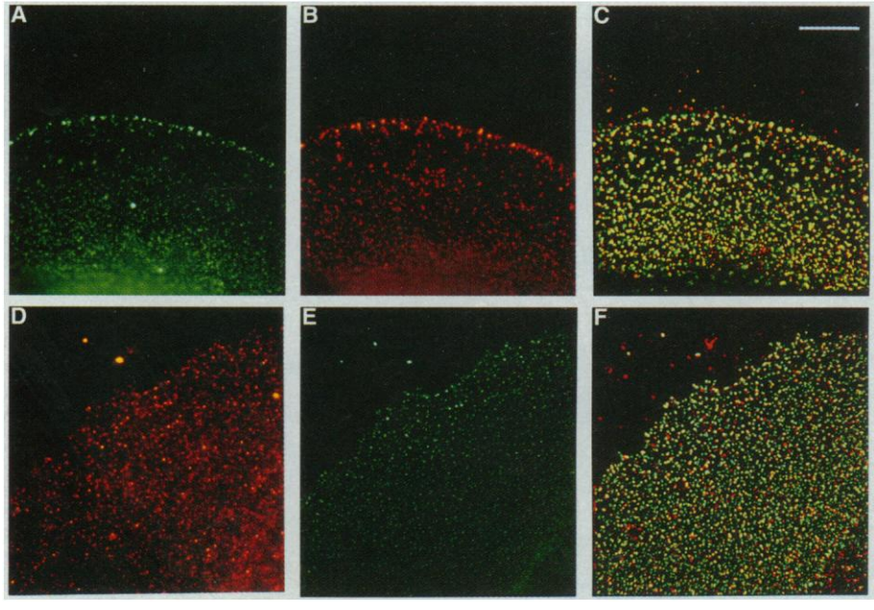

Fig. 4. Coclustering of GPI-anchored proteins and association with caveolae. (**A** to **C**) Cells of the CaCo-2 line were incubated with polyclonal rabbit anti-folate receptor IgG (15 μg/ml) and FITC-labeled mouse anti-DAF followed by rhodamine-conjugated anti-rabbit IgG (25 μg/ml) and unlabeled polyclonal goat anti-mouse IgG and imaged as described (*26*). The green color in (A) represents DAF fluorescence, while red color in (B) represents folate receptor fluorescence. (C) The images from (A) and (B) were processed to identify punctate foci (*13*), which were then substituted with a single intensity value. The two processed images (red and green) were superimposed and photographed directly from the monitor. This procedure allows easy visualization of the colocalization of folate receptor and DAF in CaCo-2 cells; yellow foci represent colocalized clusters. (**D** to **F**) Cells of the CaCo-2 line were treated with polyclonal rabbit anti-folate receptor IgG followed by fluorescein-conjugated goat anti-rabbit IgG as described above and fixed for 45 min at room temperature. The cells were then stained for caveolin and visualized with rhodamine-conjugated anti-mouse IgG as described (*8*), except that all the incubations were carried out at room temperature. (F) Images in (D) and (E) were digitally processed to allow the easy visualization of colocalization as described above. Yellow foci in panel F show colocalization of the folate receptor with caveolin. PI-PLC treatment before fixation and caveolin staining removed the folate-receptor signal, but the caveolin fluorescent pattern was unaffected (scale bar, 15 μm).

that the major pathway of internalization of the folate receptor is by way of bulk membrane endocytosis (*12, 13*) mediated by clathrin-dependent and independent pathways (*14*), similar to the pathway of other GPI-anchored proteins (*15, 16*). Previous reports that GPI-anchored proteins are excluded from coated pits (*16, 17*) may be explained by the ability of GPI-anchored proteins to redistribute to caveolae artifactually during the process of immunolocalization, thereby apparently depleting coated pits of GPI-anchored proteins.

Many cytoplasmically oriented signaling molecules, including heterotrimeric guanosine triphosphatases (GTPases), small GTPases, nonreceptor-type protein-tyrosine kinases and calcium channels and pumps, have been localized to caveolae. In addition, GPI-anchored proteins have been found in aggregates derived with Triton X-100, associated with non-receptor tyrosine kinases and other signaling molecules (*18*). The GPI-anchoring of several proteins has been shown to be important for intracellular signaling, and in most cases cross-linking of the protein is a prerequisite for their signaling function (*19*). Our data suggest that cross-linking the diffusely distributed GPI-anchored proteins could bring these proteins into caveolae in which they would interact with signal-generating proteins. The physiological activators of clustering GPI-anchored proteins are not known, and as with receptor-activated tyrosine kinases [such as epidermal growth factor receptor (*20*)], cross-linking may be the means to activate signaling.

Recently, caveolin has been localized to the cytoplasmic surface of the trans-Golgi network (TGN) and secretory vesicles (*21*). Selective domain formation and aggregation in the TGN have been implicated in the polarized sorting of proteins to the apical surface (*22*) or the sorting of proteins to secretory granules (*23*). Thus, the preferential localization of cross-linked GPI-anchored proteins to caveolin-coated areas of membranes may lead to the formation of GPI-rich domains leading to their observed polarized distribution, regulated sorting, or both. The ability to modulate the extent of oligomerization of GPI-anchored proteins in caveolin-coated areas of the cell may be important for the selective trafficking of GPI-anchored proteins.

REFERENCES AND NOTES

1. M. G. Low, *Biochim. Biophys. Acta* **988**, 427 (1989); G. A. M. Cross, *Annu. Rev. Cell Biol.* **6**, 1 (1990); M. C. Field and A. K. Menon, in *Lipid Modification of Proteins*, M. J. Schlesinger, Ed. (CRC Press, Boca Raton, FL, 1992), pp. 83–134; P. T. Englund, *Annu. Rev. Biochem.* **62**, 121 (1993).
2. R. G. W. Anderson, B. A. Kamen, K. G. Rothberg, S. W. Lacey, *Science* **255**, 410 (1992).
3. L. R. Coney *et al.*, *Cancer Res.* **51**, 6125 (1991).
4. S. W. Lacey *et al.*, *J. Clin. Invest.* **84**, 715 (1989).
5. K. G. Rothberg *et al.*, *J. Cell Biol.* **110**, 637 (1990).
6. Y. Ying, R. G. W. Anderson, K. G. Rothberg, *Cold Spring Harbor Symp. Quant. Biol.* **57**, 593 (1992).
7. The extent of colocalization was determined as described previously (*13*). The extent of random colocalization for each pair of images was estimated by translating one of a pair of images shifted 7 μm in the *x* and *y* dimensions with respect to the other and then determining the amount of colocalization. This procedure gives an accurate measure of random overlap of similar numbers of spots as contained in the aligned images. Random colocalization values were found to be 24% for the folate receptor colocalization with DAF and 14% for DAF colocalization with folate receptor (Fig. 4, A to C).
8. K. G. Rothberg *et al.*, *Cell* **68**, 673 (1992).
9. ———, Y.-S. Ying, B. A. Kamen, R. G. W. Anderson, *J. Cell Biol.* **111**, 2931 (1990).
10. X.-X. Xu and I. Tabas, *J. Biol. Chem.* **266**, 17040 (1991).
11. R. G. W. Anderson, *Trends Cell Biol.* **3**, 69 (1993).
12. G. Griffiths, R. Back, M. Marsh, *J. Cell Biol.* **109**, 2703 (1989).
13. S. Mayor, J. P. Presley, F. R. Maxfield, *ibid.* **121**, 1257 (1993).
14. B. van Deurs, P. K. Holm, K. Sandvig, S. H. Hansen, *Trends Cell Biol.* **3**, 249 (1993).
15. R. A. van den Bosch *et al.*, *EMBO J.* **7**, 3345 (1988); C. C. Widnell *et al.*, *Cell* **28**, 61 (1982).
16. G.-A. Keller, M. W. Siegel, I. W. Caras, *EMBO J.* **11**, 863 (1991).
17. M. S. Bretscher, J. N. Thomson, B. M. F. Pearse, *Proc. Natl. Acad. Sci. U.S.A.* **77**, 4156 (1980).
18. I. Štefanová *et al.*, *Science* **254**, 1016 (1991); M. Sargiacomo *et al.*, *J. Cell Biol.* **122**, 789 (1993); T. Fujimoto *et al.*, *ibid.* **119**, 1507 (1992); T. Fujimoto, *ibid.* **120**, 1147 (1993).
19. P. J. Robinson, *Immunol. Today* **12**, 35 (1991); D. Brown, *Curr. Opin. Immunol.* **5**, 349 (1993); M. A. J. Ferguson, *Parasitol. Today* **10**, 48 (1994).
20. A. Ullrich and J. Schlessinger, *Cell* **61**, 203 (1990).
21. P. Dupree *et al.*, *EMBO J.* **12**, 1597 (1993).
22. K. Simons and A. Wandinger-Ness, *Cell* **62**, 207 (1990).
23. R. B. Kelly, *Science* **230**, 25 (1985).
24. The fluorescent labeling of mAbs and labeling of cells on cover-slip dishes were carried out as described in previous reports [(*13*), and references therein]. Cells of the G3G2 line were grown on cover slip dishes in Dulbeco's minimal essential medium (DMEN) containing 10% calf serum and Geneticin (500 μg/ml) [DMEM-FBS (fetal bovine serum); Gibco-BRL]. The cells were preincubated in Hepes-buffered F-12 medium containing 0.2% bovine serum albumin (HF-BSA) at 37°C for 10 min before incubation with primary antibodies at 10 μg/ml and 37°C for 8 min, and rinsed in warm HF-BSA. The living cells were maintained at 34°C on the microscope stage with the use of a stage warmer. Fluorescence microscopy and digital image collection were performed with a Leitz Diavert (Wetzlar, Germany) fluorescence microscope with a Photometrics cooled charge-coupled device camera. The images were directly photographed from the monitor. To confirm that the fluorescence was specific to GPI-anchored forms of the proteins in question, phosphatidylinositol-specific phospholipase (PI-PLC, from *Bacillus thuringiensis*) digestion (10 U/ml, 1 hour at 23°C) was performed on cells stained with fluorescently labeled antibodies. Under these conditions, PI-PLC released almost all the fluorescence from the cells.
25. Cells of the MA104 strain were maintained in folate-deficient DMEM-FBS and plated on coverslip dishes 5 days before the experiment. All incubations on fixed cells were carried out at room temperature. For the electron microscopic studies, the labeling of live cells with secondary antibodies and gold-labeled antibodies was carried out at 4°C, and after the rinsing of unbound antibodies, the cells were incubated an additional 10 min at 37°C. The cells were then processed for electron microscopy as described previously (*5*). Species-specific polyclonal IgGs to primary antibodies were obtained from Pierce Chemical (Rockford, IL). Affinity-purified rabbit polyclonal IgG for folate receptor was obtained as described previously (*5*). Gold-conjugated antibodies were obtained from EY Laboratories (San Mateo, CA).
26. Cells of the CaCo-2 line were maintained in DMEM-FBS and plated on cover-slip dishes 3 to 5 days before the experiment. HUVECS were isolated as described [A. J. Huang *et al.*, *J. Cell Biol.* **120**, 1371 (1993)] and maintained in DMEM-FBS. The cells were pre-incubated in HF-BSA at 0°C for 10 min before incubation with primary antibodies at 10 to 15 μg/ml for 45 min at 0°C, rinsed in HF-BSA, and incubated for an additional 45 min at 0°C in the presence or absence of appropriate secondary antibody at 10 to 30 μg/ml. In each case, all the fluorescence associated with the cells could be released by the treatment of the cells with PI-PLC at 10 units/ml for 1 hour at room temperature. Mouse mAb to DAF (1A10) [M. Davitz *et al.*, *J. Exp. Med.* **163**, 1150 (1986)] was from the author of the preceding work. Rat mAb to Thy-1.2 was purchased from Gibco-BRL.
27. Pre-fix and post-fix refer to the fixation routine used for the detection of the primary antibody as described in Fig. 1, C and D, respectively. Non-specific binding of gold particles to MA104 cells was determined for the two conditions described in Fig. 1, C to E, with an isotype-matched IgG (MOPC-21, Sigma) as the primary antibody. Less than 0.02 gold particle per micrometer was detected in either case. A cluster was defined to contain more than three gold particles separated by less than 50 nm from the nearest neighbor. Gold particles (or clusters) less than 50 nm from the edge of caveolae or coated pits were considered to be associated with them. To be consistent with previous electron microscopic analyses, we have used similar criteria as previously described (*5, 6*). Of the 17 clusters obtained in the two pre-fix cases, only one was found associated with a caveola. The relative concentration is the ratio of the observed gold particle density in caveolae or coated pits to the expected gold particle density over these structures. The expected gold particle density over caveolae or coated pits is the product of the gold particle density per unit length and the total length of membrane associated with these structures. The average membrane length associated with caveolae and coated pits was 0.15 μm and 0.25 μm, respectively.

28. We thank M. Low for a generous gift of *B. thuringienses* PI-PLC, R. G. W. Anderson and Centocor Corporation (Malvern, PA) for mouse mAb to folate receptor (MOv19), M. Davitz for mouse mAb to DAF (1A10), J. Glenny (Glentech, Lexington, KY) for anti-caveolin monoclonal IgG, D. Gelman for excellent assistance with photography, and P. Leopold and K. Brown for their excellent help with electron microscopy. S.M. would like to thank A. Lorde and F. F. Bosphorus for inspiration. Supported by a grant from the Helen Hay Whitney Foundation (S.M.) and NIH grant DK27083 (F.R.M.).

3 February 1994; accepted 6 May 1994